

2.3 Statistical Structure of Global Significant Wave Heights

Peter C. Chu¹⁾ George Galanis²⁾, Yu-Heng Kuo¹⁾
¹⁾Naval Postgraduate School, Monterey, California, USA
²⁾Naval Academy of Greece, Piraeus, Greece

Abstract

Near-real time ocean significant wave heights from ERS-1 & 2, Topex/Poseidon, Geosat Follow-on, Jason-1 and 2, and Envisat on $1^\circ \times 1^\circ$ resolution for world oceans (82.5° S to 82.5° N) are available online as “Radar Altimetry Tutorial (RAT)”. The probability distribution function (PDF) of the significant wave heights (w), constructed from global RAT data from 2005 to 2009, satisfies the two-parameter Weibull distribution reasonably well. Knowledge on PDF of w will improve the ensemble flux calculation across the air-ocean interface, which contributes to the climate studies.

1. Introduction

Fluxes of momentum, heat, moisture, and chemical constituents across the air-ocean interface influence on the global redistribution of heat and in turns on the global climate change. Without ocean waves, the atmospheric marine boundary layer is above an infinite, flat surface. With ocean waves, such a treatment is no longer valid; the concept of wave boundary layer should be applied. In the wave boundary layer, the air-ocean fluxes are affected by waves through changing the surface parameters such as exchange coefficients (such as the drag coefficient C_D), roughness length z_0 , and air-sea transfer velocity of individual chemical constituent (Chu and Cheng 2007), i.e., the surface parameters (i.e., C_D , z_0 , ...) depend on wave characteristics. The significant wave height (SWH) is the mean of the highest one-third of the waves and represents a major wave feature. Knowledge on statistical structure of SWH leads to more accurate calculation of fluxes across the air-ocean interface with the ocean wave propagation. Thus, there is a need for determination of the probability distribution function (PDF) of SWH.

¹⁾ Corresponding author address: Peter C. Chu, Naval Postgraduate School, Monterey, CA 93943, email: pcchu@nps.edu

The Weibull model has been proposed for SWH from analyzing wave buoy data for regional areas such as in the eastern Arabian Sea (Muraleedharan et al. 2007). Question arises: Can such a result (e.g., the Weibull distribution for the eastern Arabian Sea SWH) be extended to global oceans? To answer this question, we use the daily data from Radar Altimetry Tutorial (RAT) (<http://www.altimetry.info/>) from 11 December 2005 to 24 July 2009 to construct the observational PDF of SWH for the global oceans. Special characteristics of the statistical parameters such as mean, standard deviation, skewness, and kurtosis will also be identified.

2. Radar Altimetry Tutorial

RAT provides merged SWH data from ERS-1 & 2, Topex/Poseidon, Geosat Follow-on, Jason-1 and 2, and Envisat (Rosmorduc et al. 2009). The data are available for the world oceans from 82.5° N to 82.5° S on $1^\circ \times 1^\circ$ grid to a broad-based user community via a web-based interactive data selection interface on daily base starting from 11 December 2005. The near real-time product is based on the last two days of data available for each satellite from which a merged map is generated if a minimum of two missions are available. Data are cross-calibrated using Jason-1 as reference mission. The resulting map is improved in case of additional mission availability. See website: [http://www.altimetry.info/documents/Radar Altimetry Tutorial 20090406.pdf](http://www.altimetry.info/documents/Radar_Altimetry_Tutorial_20090406.pdf) for detailed information. In this study, we first use the global SWH data from 11 December 2005 to 24 July 2009 to get overall statistical features; and then use the North Atlantic SWH data for the whole year of 2008 to obtain seasonal variation of the SWH statistical structures, which can be used for numerical wave model verification.

3. Descriptive Statistics of SWH

In this section the main descriptive statistical results for the data in study are presented. A variety of indexes has been adapted capturing different aspects of the data evolution and

revealing, in this way, both the main characteristics of observational and forecasted data as well as their main differences. More precisely, the following statistical measures are employed: mean, standard deviation (std), coefficient of variance (cv), skewness, and kurtosis:

$$\begin{aligned} \text{mean}(w) &= \frac{1}{N} \sum_{i=1}^N w_i, \\ \text{std}(w) &= \sqrt{\text{mean}[w - \text{mean}(w)]^2}, \\ \text{cv} &= \frac{\text{std}}{\text{mean}}, \\ \text{skew}(w) &= \frac{\text{mean}\{[w - \text{mean}(w)]^3\}}{\text{std}^3(w)}, \\ \text{kurt}(w) &= \frac{\text{mean}\{[w - \text{mean}(w)]^4\}}{\text{std}^4(w)} - 3. \end{aligned} \quad (1)$$

The five parameters (mean, standard deviation, coefficient of variance, skewness, and kurtosis) are calculated from the observational SWH from 11 December 2005 to 24 July 2009 for the each grid point. The mean, standard deviation, skewness, and kurtosis fields of SWH estimated from the RAT data are displayed in Figs. 1-4.

Large values of mean SWH occur in the Southern Ocean with maximum values higher than 5 m. Next high mean SWH areas are in the northern parts of the Gulf Stream and Kuroshio Extension regions with maximum values around 3-3.5 m. The mean SWH is low in regional seas (Fig. 1). Large standard deviation of SWH is in the North Atlantic and North Pacific (north of 30° N) with maximum value higher than 1.6 m, and in the Southern Ocean with maximum value around 1.2 m. Low standard deviation of SWH is in the tropical regions (Fig. 2). In general, SWH is positively skewed everywhere in the global oceans with high skewness in mid-latitudes and western boundary regions with maximum value higher than 1.6 and with low skewness in the tropical regions and Southern Ocean (Fig. 3). The kurtosis of SWH exceeds 1.9 everywhere with large values in the mid-latitudes and western boundary regions in world oceans (Fig. 4). The characteristics of skewness and kurtosis show that the SWH does not satisfy the Gaussian distribution.

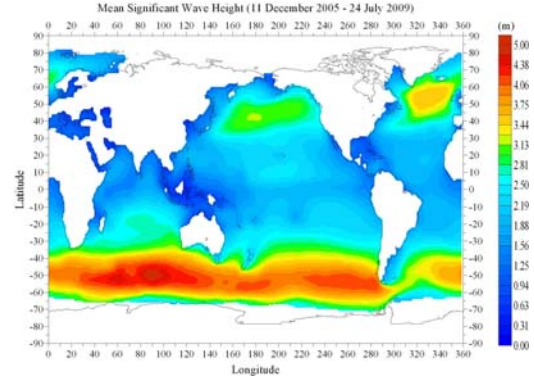


Fig. 1. Mean SWHs calculated from the RAT data (11 December 2005 – 24 July 2008).

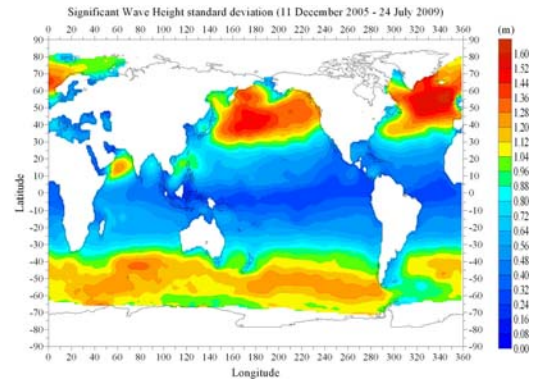


Fig. 2. Standard deviation of global SWHs calculated from the RAT data (11 December 2005 – 24 July 2008).

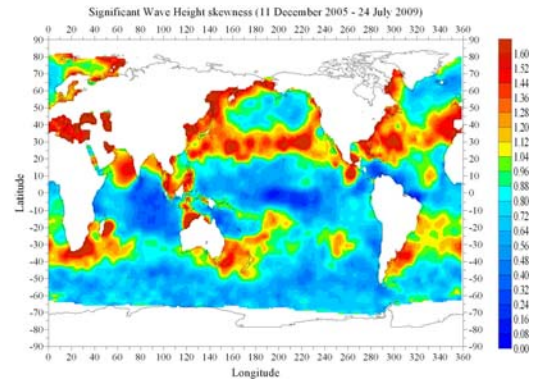


Fig. 3. Skewness of global SWHs calculated from the RAT data (11 December 2005 – 24 July 2008).

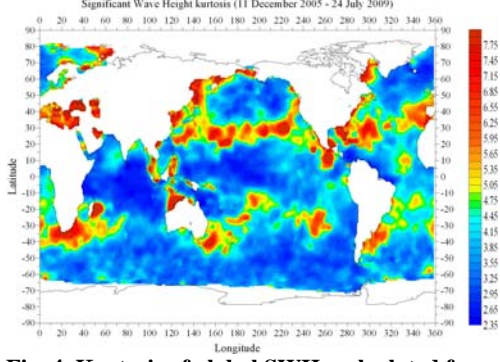


Fig. 4. Kurtosis of global SWHs calculated from the RAT data (11 December 2005 – 24 July 2008).

3. Parameters of the Weibull Distribution

The Weibull probability density function of a random variable w is given by

$$p(w) = \frac{b}{a} \left(\frac{w}{a}\right)^{b-1} \exp\left[-\left(\frac{w}{a}\right)^b\right], \quad (2)$$

where the parameters a and b denote the scale and shape of the distribution. This distribution has been recently used in investigating the ocean surface current speeds (Chu, 2008, 2009). The four parameters (mean, standard deviation, skewness, and kurtosis) of the Weibull distribution are calculated by (Johnson et al. 1994),

$$\text{mean}(w) = a\Gamma\left(1 + \frac{1}{b}\right), \quad (3)$$

$$\text{std}(w) = a \left[\Gamma\left(1 + \frac{2}{b}\right) - \Gamma^2\left(1 + \frac{1}{b}\right) \right]^{1/2}, \quad (4)$$

where Γ is the gamma function. The parameters a and b can be inverted (Monahan 2006) from (3) and (4),

$$b = \left[\frac{\text{mean}(w)}{\text{std}(w)} \right]^{1.086}, \quad a = \frac{\text{mean}(w)}{\Gamma(1 + 1/b)}. \quad (5)$$

The skewness and kurtosis are computed by

$$\text{skew}(w) = \frac{\Gamma\left(1 + \frac{3}{b}\right) - 3\Gamma\left(1 + \frac{1}{b}\right)\Gamma\left(1 + \frac{2}{b}\right) + 2\Gamma^3\left(1 + \frac{1}{b}\right)}{\left[\Gamma\left(1 + \frac{2}{b}\right) - \Gamma^2\left(1 + \frac{1}{b}\right) \right]^{3/2}} \quad (6)$$

$$\text{kurt}(w) = \frac{\Gamma\left(1 + \frac{4}{b}\right) - 4\Gamma\left(1 + \frac{1}{b}\right)\Gamma\left(1 + \frac{3}{b}\right)}{\left[\Gamma\left(1 + \frac{2}{b}\right) - \Gamma^2\left(1 + \frac{1}{b}\right) \right]^2} + \frac{6\Gamma^2\left(1 + \frac{1}{b}\right)\Gamma\left(1 + \frac{2}{b}\right) - 3\Gamma^4\left(1 + \frac{1}{b}\right)}{\left[\Gamma\left(1 + \frac{2}{b}\right) - \Gamma^2\left(1 + \frac{1}{b}\right) \right]^2} - 3, \quad (7)$$

which depend on the parameter b only [see (6) and (7)] for the Weibull distribution. The relationship between the kurtosis and skewness can be determined from (6) and (7), i.e.,

$$\text{kurt} = F(\text{skew}). \quad (8)$$

The relationship between $\text{kurt}(w)$ and $\text{skew}(w)$ can be used to identify the fitness of the Weibull distribution for observational w -PDFs. The solid curve on these figures shows the relationship for a Weibull variable. Fig. 5 shows the kernel density estimates of joint PDF of $\text{kurt}(w)$ versus $\text{skew}(w)$ for the RAT data from 2005 to 2009. The contour intervals are logarithmically spaced. The thick black line is the theoretical curve for a Weibull variable. The relationship between $\text{skew}(w)$ and $\text{kurt}(w)$ in the observations is similar to that for a Weibull variable with smaller kurtosis.

4. Seasonal Variation of Statistical Parameters

The SWH data from RAT for the North Atlantic (0-80N, 100W – 30E) in 2008 with was used to calculate the statistical parameters. The sample size exceeds 2 million values. Monthly values of these parameters were computed and then grouped into two categories: “Summer” (April-September) and “Winter” months (October-March) (Table -1). The range of SWH values are increased during winter, as well as the

corresponding mean value and variability. On the contrary, the increased kurtosis during summer months, reveals that a significant part of the variability is related to non frequent outliers. The percentiles are presented in Table 2. The two scale parameters of the Weibull distribution are listed in Table 3.

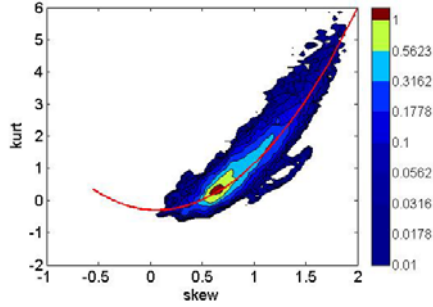


Fig. 5. Kernel density estimates of joint PDFs of skew(w) and kurt(w) from the RAT data during 11 December 2005 to 24 July 2009. The contour intervals are logarithmically spaced. The thick black line is the theoretical curve for a Weibull variable.

Table 1. The main statistical parameters from RAT data summarized for the whole 2008, the summer and winter months.

| Statistical Parameter | Over All | Summer | Winter |
|-----------------------|----------|--------|--------|
| Range | 6.61 | 5.60 | 7.61 |
| Mean | 2.14 | 1.71 | 2.57 |
| Std. | 1.02 | 0.76 | 1.28 |
| Coeff. of Variation | 0.47 | 0.44 | 0.50 |
| Skewness | 1.09 | 1.05 | 1.14 |
| Kurtosis | 1.91 | 2.47 | 1.35 |

Table 2. Percentiles from RAT data for the whole 2008, the summer and winter months.

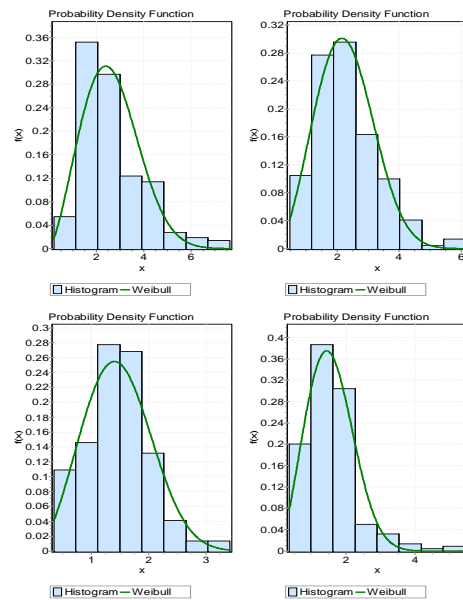
| Percentile | OverAll | Summer | Winter |
|----------------------|---------|--------|--------|
| P_5 | 0.82 | 0.65 | 0.98 |
| P_{10} | 1.04 | 0.84 | 1.24 |
| $P_{25}=Q1$ | 1.44 | 1.21 | 1.67 |
| P_{50} (Median) | 1.94 | 1.62 | 2.26 |
| $P_{75}=Q3$ | 2.65 | 2.10 | 3.20 |
| P_{90} | 3.53 | 2.66 | 4.39 |
| P_{95} | 4.12 | 3.10 | 5.13 |

Table 3. Weibull parameters from RAT data for the whole study period, the summer and winter months

| Weibull Parameters | Summer | Winter | OverAll |
|--------------------|--------|--------|---------|
| b | 2.61 | 2.51 | 2.56 |
| a | 1.89 | 2.83 | 2.36 |

5. Observational PDF

Fig. 6 shows the well fitting of the SWH data to the Weibull distributions is further sustained by the use of histograms of the data in comparison with the corresponding (bi-monthly) Weibull probability density function. The probability-probability (P-P) plot is a graph of the empirical Cumulative Distribution Function (CDF) values plotted against the theoretical CDF values (Fig. 7). On the other hand, the quantile-quantile (Q-Q) plot is a graph of the input (observed) data values plotted against the theoretical (fitted) distribution quantiles (Fig. 8). Both axes of these graphs are in units of the input data set. PP and QQ plots will be approximately linear if the specified theoretical distribution is the correct model. The corresponding PP and QQ plots (Figures 7, 8) show that the SWH fits the Weibull distribution.



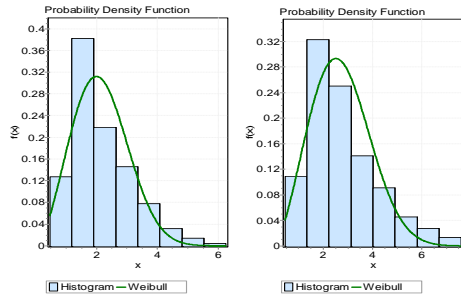


Fig. 6. Histograms of the SWH data in comparison with the Weibull probability density functions for (a) February, (b) April, (c) June, (d) August, (e) October, and (f) December.

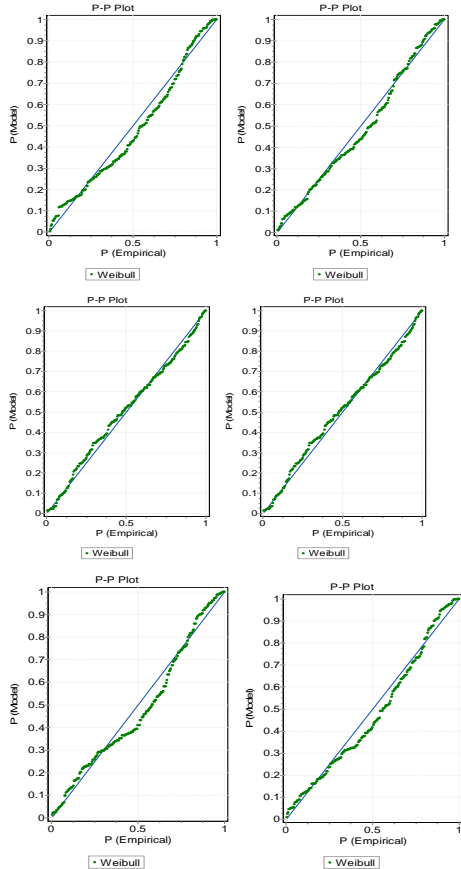


Fig. 7. P-P plot of the SWH data with the Weibull probability density functions for (a) February, (b) April, (c) June, (d) August, (e) October, and (f) December.

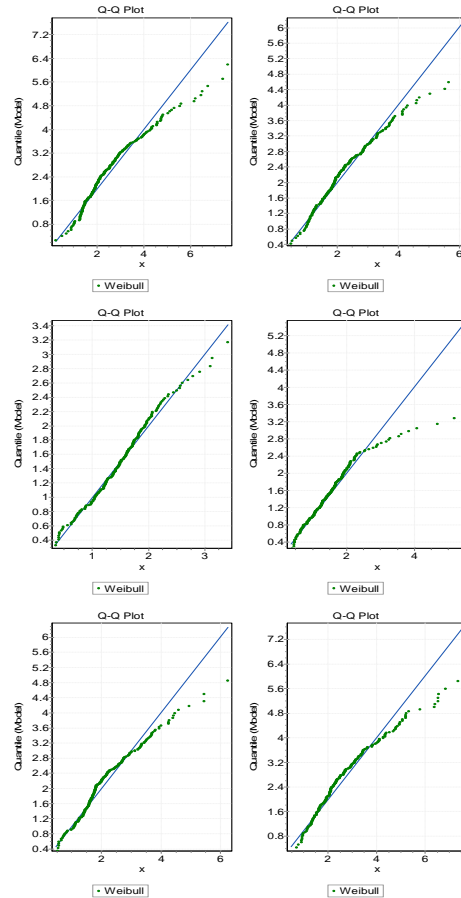


Fig. 8. Q-Q plot of the SWH data with the Weibull probability density functions for (a) February, (b) April, (c) June, (d) August, (e) October, and (f) December.

The agreement between the moment relationships in the RAT data and those for a Weibull variable and P-P, Q-Q plots reinforce the conclusion that these data are Weibull to a good approximation.

6. Conclusions

This study has investigated the probability distribution function of the global significant wave heights (w), using long-term RAT data. The following results were obtained.

(1) Probability distribution function of the global significant wave heights approximately satisfies the two-parameter Weibull distribution.

(2) Four moments of w (mean, standard deviation, skewness, kurtosis) have been characterized. Large mean SWH occur in the Southern Ocean with maximum values higher than 5 m. Large standard deviation of SWH is in the North Atlantic and North Pacific (north of 30° N) with maximum value higher than 1.6 m. The SWH is positively skewed everywhere in the global oceans. The kurtosis of SWH exceeds 1.9 everywhere with large values in the mid-latitudes and western boundary regions in world oceans.

(3) The relationship between skew(w) and kurt(w) from the data is in fairly well agreement with the theoretical Weibull distribution. The histograms, P-P plots and Q-Q plots show the same results.

(4) The Weibull distribution provides a good empirical approximation to the PDF of global ocean significant wave heights with strong seasonal variation. This may improve the representation of the fluxes across the air-ocean interface, which in turn impact on the coupled air-ocean dynamics of the climate system.

Acknowledgments

This research was supported by the Office of Naval Research, Naval Oceanographic Office, and Naval Postgraduate School.

References

Chu, P.C., 2008: Probability distribution function of the upper equatorial Pacific current speeds. *Geophysical Research Letters*, **35**, doi:10.1029/2008GL033669.

Chu, P. C., 2009: Statistical Characteristics of the Global Surface Current Speeds Obtained from Satellite Altimeter and Scatterometer Data. *IEEE Journal of Selected Topics in Earth Observations and Remote Sensing*, **2** (1), 27-32

Chu, P.C., and K.F. Cheng, 2007: Effect of wave boundary layer on the sea-to-air dimethylsulfide transfer velocity during typhoon passage. *Journal of Marine Systems*, **66**, 122-129.

Johnson, N., S. Kotz, and N. Balakrishnan, 1994: Continuous Univariate Distributions. Vol. 1. Wiley, 756 pp.

Monahan, A.H., 2006: The probability distribution of sea surface wind speeds. Part-1: theory and SeaWinds observations. *Journal of Climate*, **19**, 497-519.

Muraleedharan, G., A.D. Rao, P.G. Kurup, N. U. Nair, and M. Sinha, 2007: Modified Weibull distribution for maximum and significant wave height simulation and prediction. *Coastal Engineering*, **54**, 630-638.

Rosmorduc, V., J. Benveniste, O. Lauret, C. Maheu, M. Milagro, and N. Picot, 2009 : Radar Altimetry Tutorial, J. Benveniste and N. Picot edited, <http://www.altimetry.info/>